Supplementary data for the article:

Cvijetić, I. N.; Tanç, M.; Juranić, I. O.; Verbić, T. Ž.; Supuran, C. T.; Drakulić, B. J. 5-Aryl-1H-Pyrazole-3-Carboxylic Acids as Selective Inhibitors of Human Carbonic Anhydrases IX and XII. *Bioorganic and Medicinal Chemistry* **2015**, *23* (15), 4649–4659.
https://doi.org/10.1016/j.bmc.2015.05.052

5-Aryl-pyrazole-3-carboxylic acids as selective inhibitors of human carbonic anhydrases IX and XII

Ilija N. Cvijetić, Muhammet Tanç, Ivan O. Juranić, Tatjana Ž. Verbić, Claudiu T. Supuran,[*] Branko J. Drakulić[**]

Table S1. Percentage of CAs I, II, IX and XII inhibition on two concentrations of compounds **1-23**

Compound	R-	Percentage of inhibition at $10^{-7}(10^{-4})$ M			
		hCA I	hCA II	hCA IX	hCA XII
1	4-Me	20 (30)	34 (35)	29 (44)	33 (48)
2	4-Et	21 (37)	35 (37)	29 (46)	41 (52)
3	4-*i*-Pr	17 (36)	31 (45)	24 (47)	33 (47)
4	4-*n*-Bu	25 (39)	35 (45)	33 (51)	42 (52)
5	4-*t*-Bu	20 (39)	36 (45)	30 (52)	41 (51)
6	2,4-di-Me	15 (32)	36 (38)	33 (50)	42 (49)
7	3,4-di-Me	19 (30)	33 (37)	28 (50)	35 (46)
8	2,4,5-tri-Me	20 (33)	33 (39)	30 (54)	35 (48)
9	2,3,5,6-tetra-Me	28 (34)	34 (41)	29 (50)	36 (46)
10	2,4,6-tri-Et	24 (33)	35 (45)	30 (49)	39 (47)
11	2,4-di-*i*-Pr	22 (44)	35 (43)	27 (52)	33 (49)
12	2,4,6-tri-*i*-Pr	17 (39)	34 (49)	26 (52)	37 (52)
13	*β*-Tetralinyl	24 (33)	19 (25)	33 (49)	43 (51)
14	*β*-Naphtyl	21 (36)	35 (38)	29 (48)	42 (54)
15	4-Phenyl	19 (34)	34 (45)	32 (48)	42 (55)
16	4-Pyrollidinyl	20 (36)	34 (48)	33 (46)	35 (52)
17	4-F	20 (29)	32 (36)	29 (45)	36 (51)
18	4-Cl	17 (30)	36 (38)	31 (45)	42 (50)
19	3-Br	20 (32)	32 (35)	30 (54)	38 (49)
20	4-OH	23 (30)	35 (41)	30 (45)	35 (51)
21	2-OMe	21 (30)	28 (40)	27 (44)	35 (50)
22	4-OMe	25 (30)	36 (40)	33 (51)	34 (47)
23	4-OMe-2,5-diMe	22 (35)	35 (40)	33 (52)	42 (47)

[*] E-mail: claudiu.supuran@unifi.it (C.T. Supuran)
[**] E-mail: bdrakuli@chem.bg.ac.rs (B.J. Drakulić)

Table S2. Calculated 3D-dependent whole-molecular properties of compounds **1**-**23** in its anionic form.

Compound	R-	SA*	PSA*	ASA*	Volume	VLog*P**
1	4-Me-	224.8130	64.0790	160.7340	177.4143	1.4671
2	4-Et-	243.2491	64.0790	179.1701	192.8189	2.0007
3	4-*i*-Pr-	264.0426	64.0790	199.9636	209.9865	2.0888
4	4-*n*-Bu-	292.9753	65.6070	227.3683	230.5539	2.8327
5	**4-*t*-Bu-**	282.4734	63.6160	**218.8573**	**228.9744**	2.6183
6	2,4-di-Me-	246.8261	65.3018	181.5243	194.0475	1.9798
7	3,4-di-Me-	242.2963	65.0251	177.2712	193.6693	1.9467
8	2,4,5-tri-Me-	264.9485	64.5335	200.4150	212.3705	2.3428
9	**2,3,5,6-tetra-Me-**	284.3445	65.9355	**218.4090**	**228.3398**	2.6140
10	2,4,6-tri-Et-	327.5655	63.9959	263.5696	261.0485	3.4748
11	2,4-di-*i*-Pr-	326.4613	64.9063	261.5551	261.1596	2.9713
12	2,4,6-tri-*i*-Pr-	387.3279	64.1751	323.1528	311.0422	3.9021
13	*β*-Tetralinyl-	268.1217	65.0251	203.0966	218.2483	2.3040
14	*β*-Naphtyl-	251.6167	64.3173	187.2994	206.9182	1.9691
15	4-Phenyl-	273.0847	64.9809	208.1038	228.0558	2.2108
16	4-Pyrrolidinyl-	281.5775	67.1797	214.3978	229.2079	1.7434
17	4-F-	205.8496	64.0790	141.7706	163.2093	1.2486
18	4-Cl-	217.0917	64.0790	153.0126	174.1838	1.6192
19	3-Br-	224.0955	64.6011	159.4944	179.5580	1.9400
20	4-OH-	211.6867	87.4045	124.2822	168.2015	0.4326
21	2-OMe-	236.4103	76.4652	159.9451	186.9544	0.9978
22	4-OMe-	232.9842	75.3840	157.6001	185.6467	1.0959
23	4-OMe-2,5-di-Me-	280.0472	75.7126	204.3346	222.4115	1.9971

*SA- Surface area, PSA - Polar surface area, ASA - Apolar surface area, Vlog*P* - Virtual log*P*

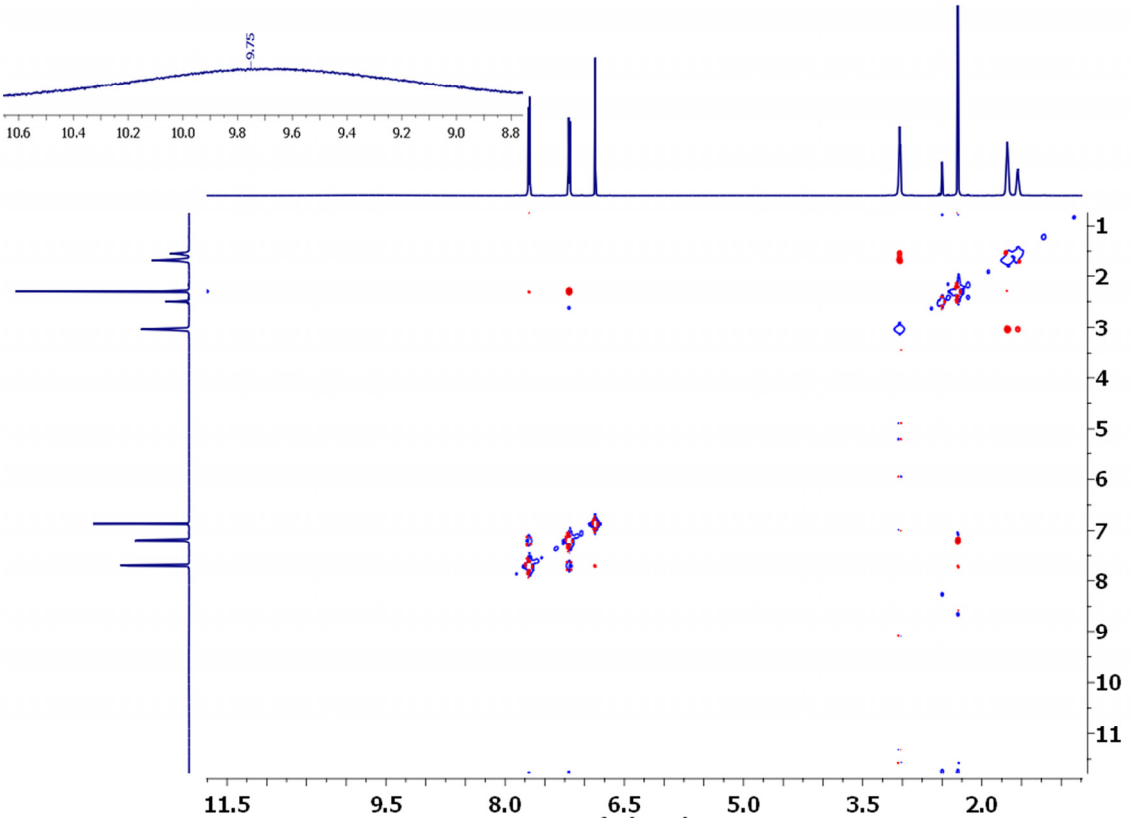

Figure S1. NOESY spectrum of 4-Me-derivative (**1**) in DMSO upon addition of the 1 molar equivalent of piperidine.

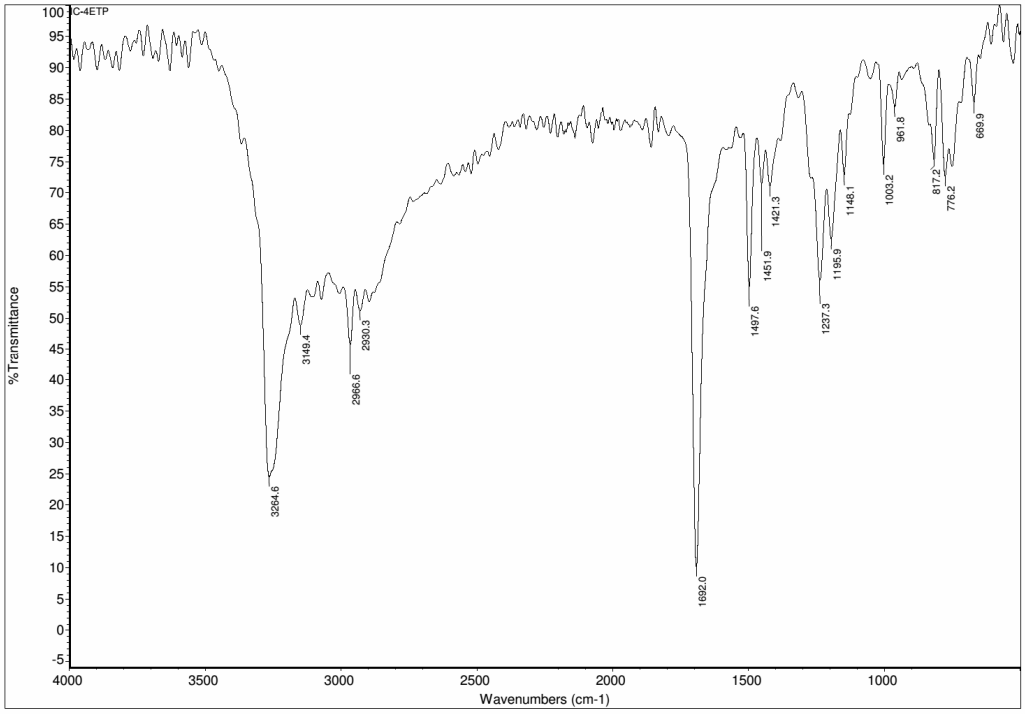

a)

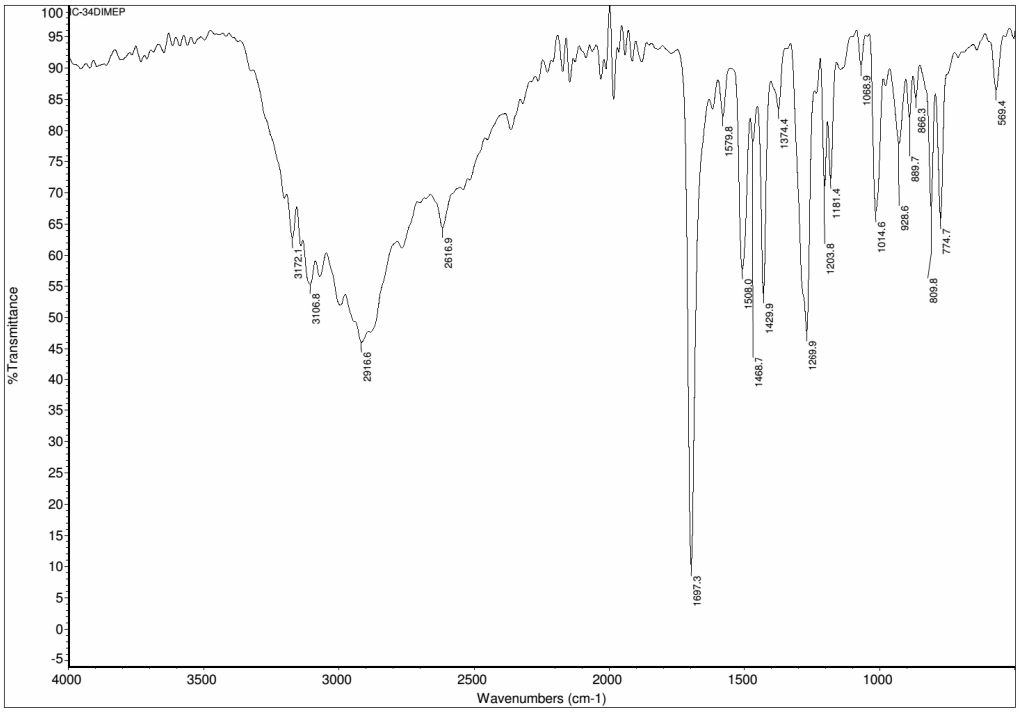

b)

Figure S2. FT-IR spectra of a) 4-Et- (**2**), and b) 3,4-di-Me-derivative (**7**). In the IR spectrum of derivative **7** broadening of N-H bands in region of ~ 3100 cm^{-1} is observed, due to aggregation by intermolecular H-bonding.

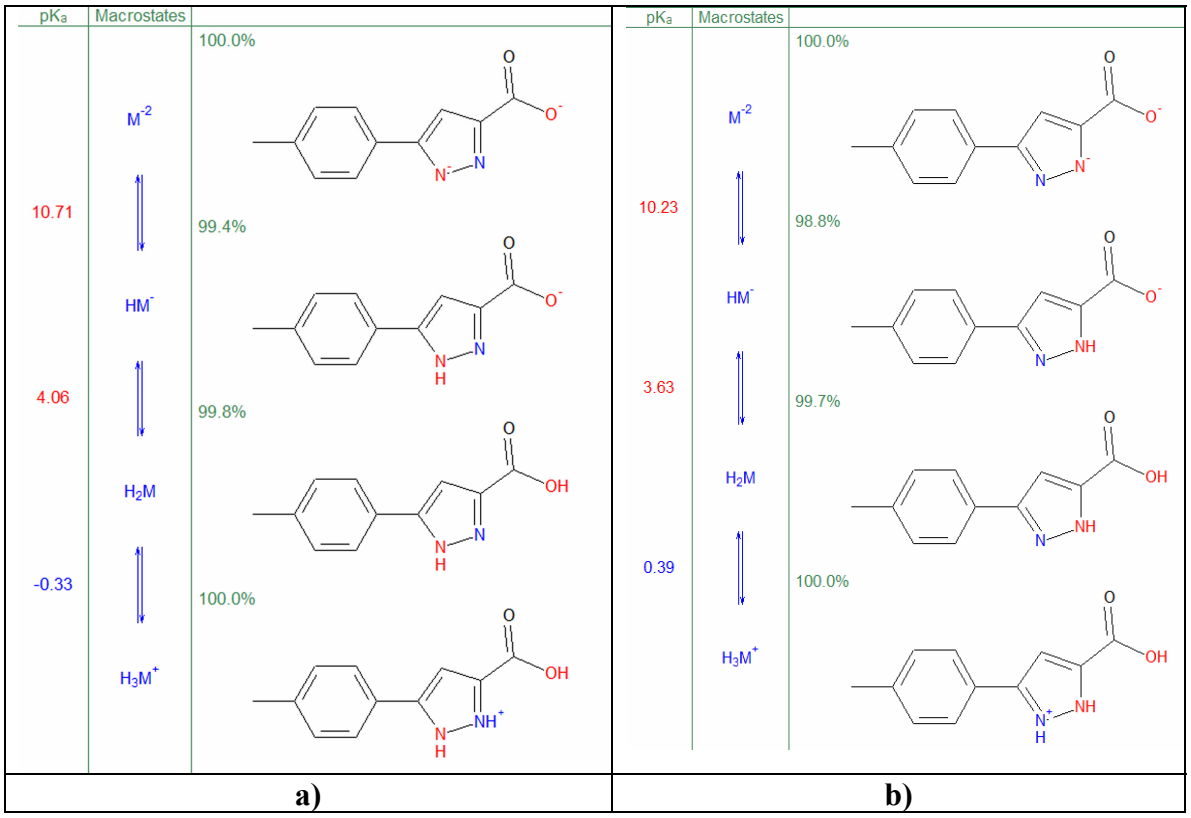

Figure S3. Estimated pK_a values of derivative **1**. Tautomers with protonated pyrazole nitrogens were used for prediction.

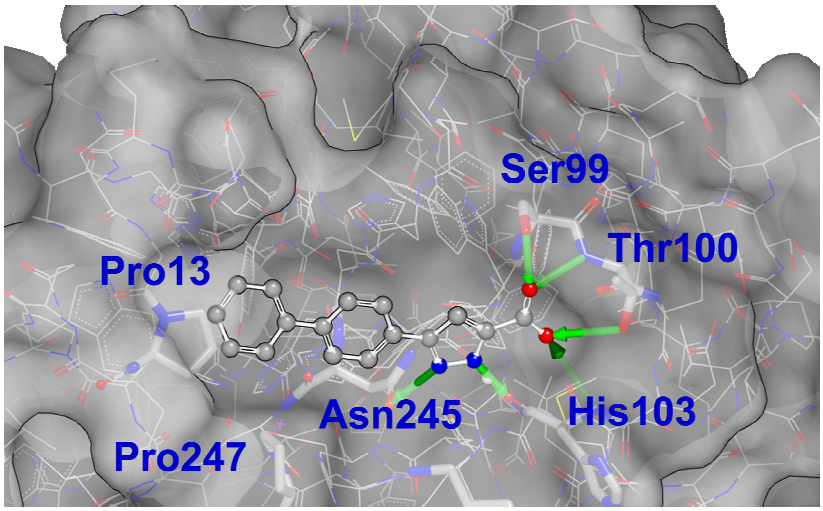

a)

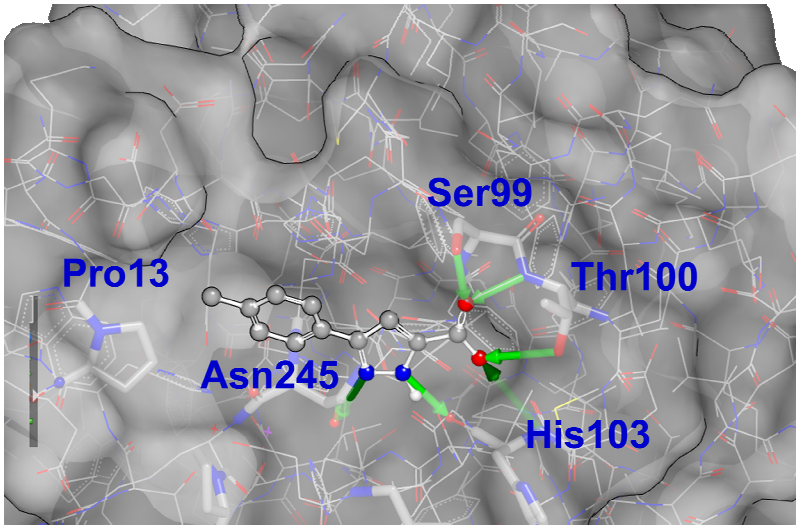

b)

Figure S4. Best-ranked solutions of compounds **15** (a) and **1**(b) docked into CA I.

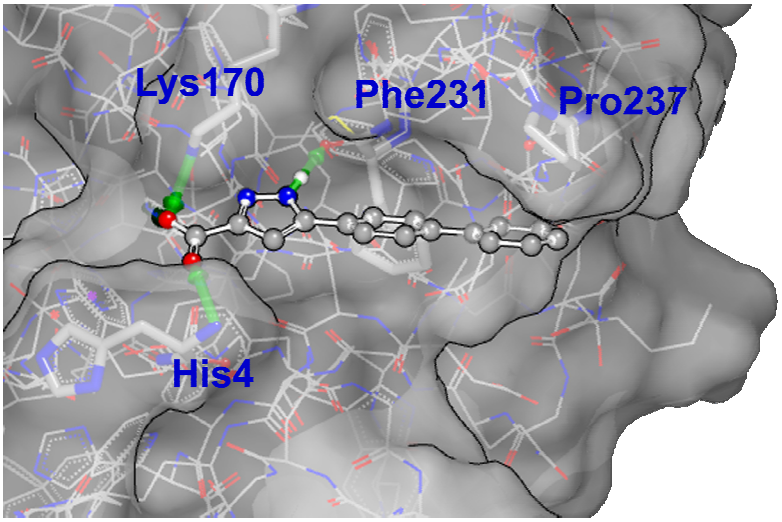

a)

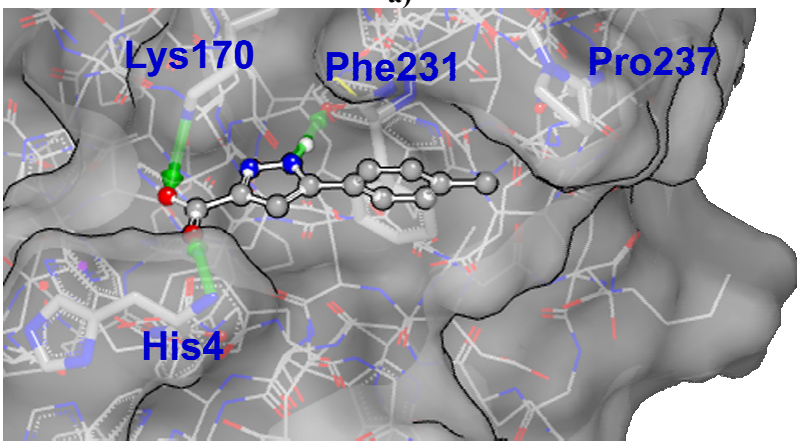

b)

Figure S5. Best-ranked solutions of compounds **15** (a) and **1**(b) docked into CA II.

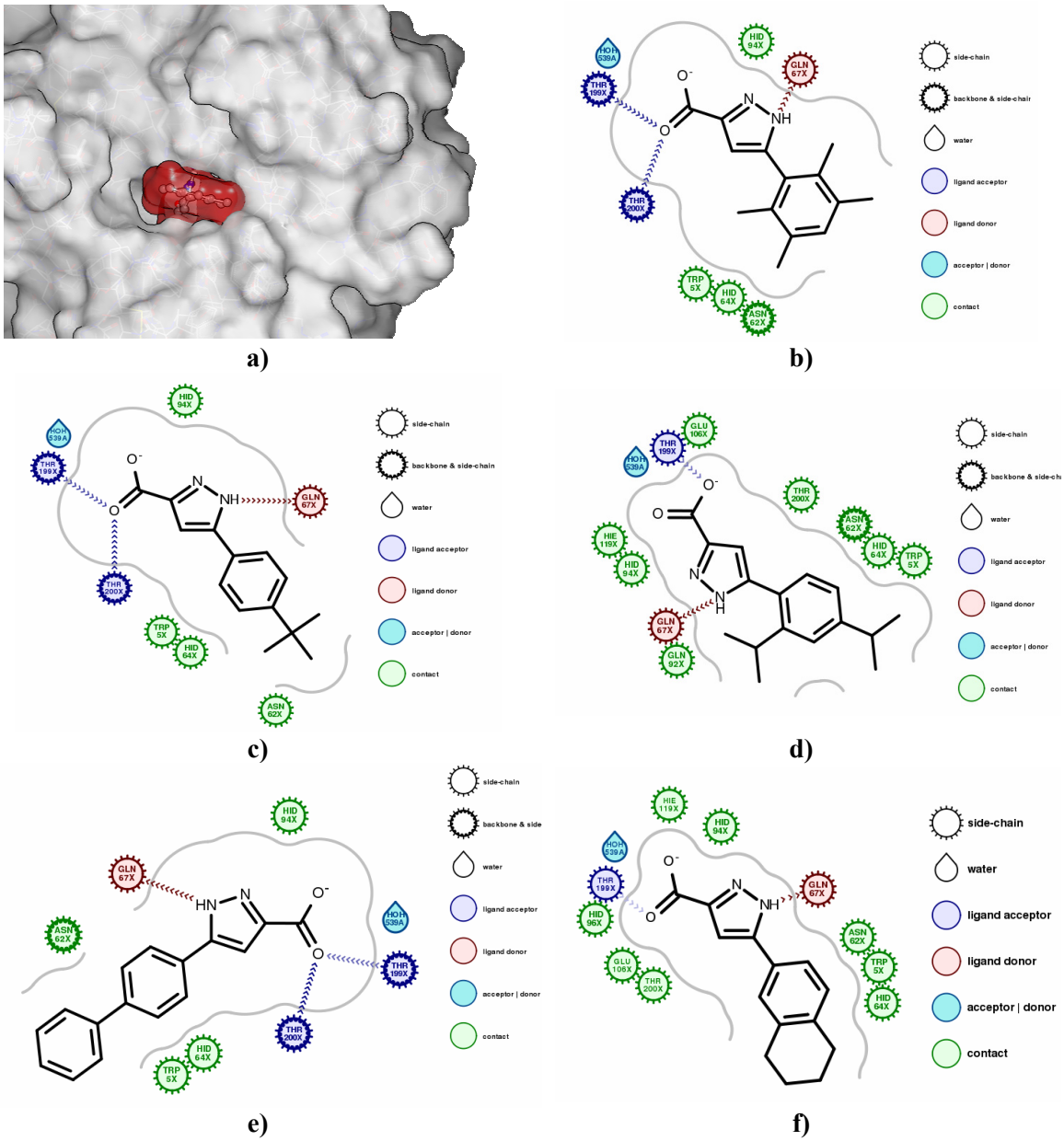

Figure S6. Shape complementarity of active and inactive compounds toward CA IX. a) Surfaces of compound **9** (red transparent) and the cleft of CAIX (gray semi-transparent) are shown. b) 2D depiction of shape complementarity of compound **9**. c) 2D depiction of shape complementarity of compound **5**. d) 2D depiction of shape complementarity of compound **11**. e) 2D depiction of shape complementarity of compound **15**. f) 2D depiction of shape complementarity of compound **13**.

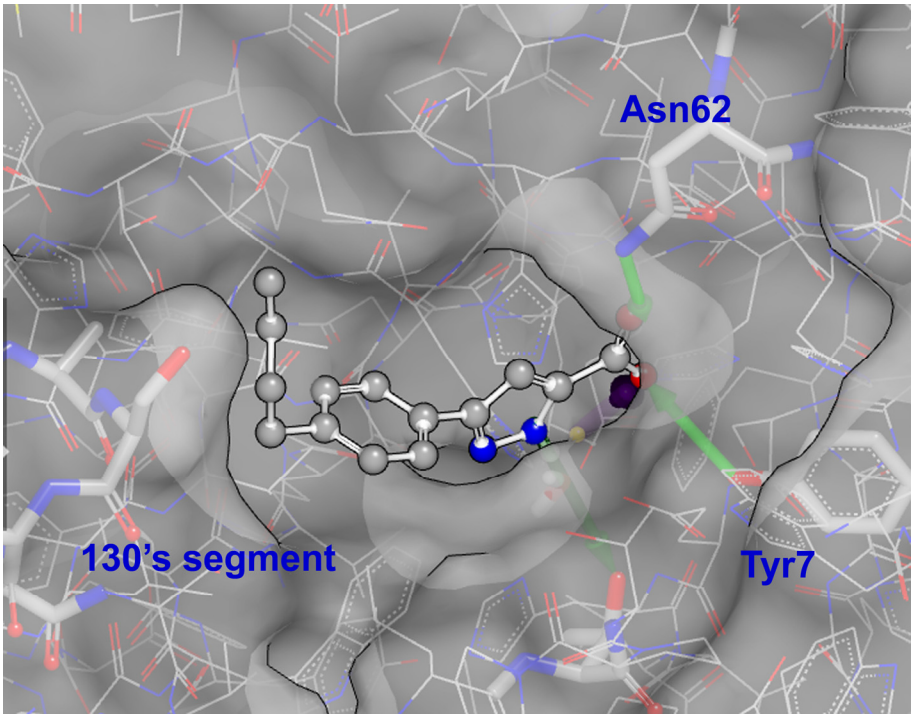
Asn62
130's segment
Tyr7

a)

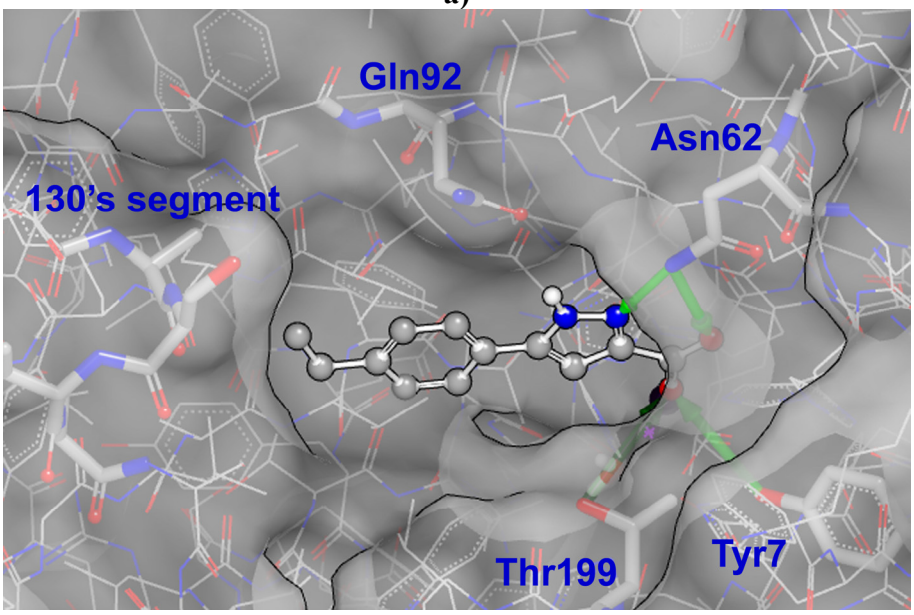
Gln92
Asn62
130's segment
Thr199
Tyr7

b)

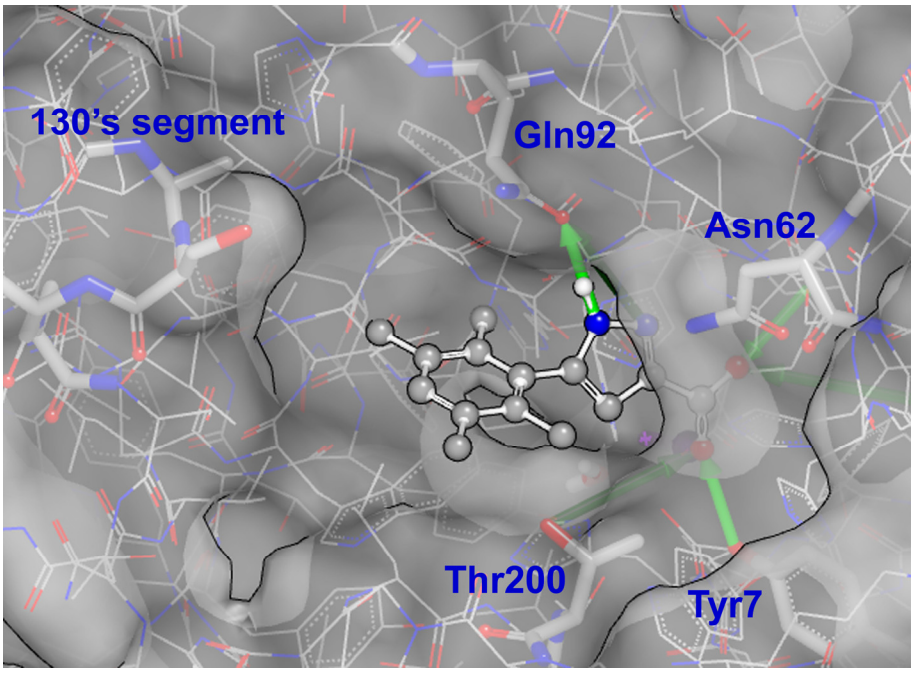

c)

Figure S7. Best-ranked solutions of compounds **4** (a), **2** (b), and **9** (c) docked into CA XII.

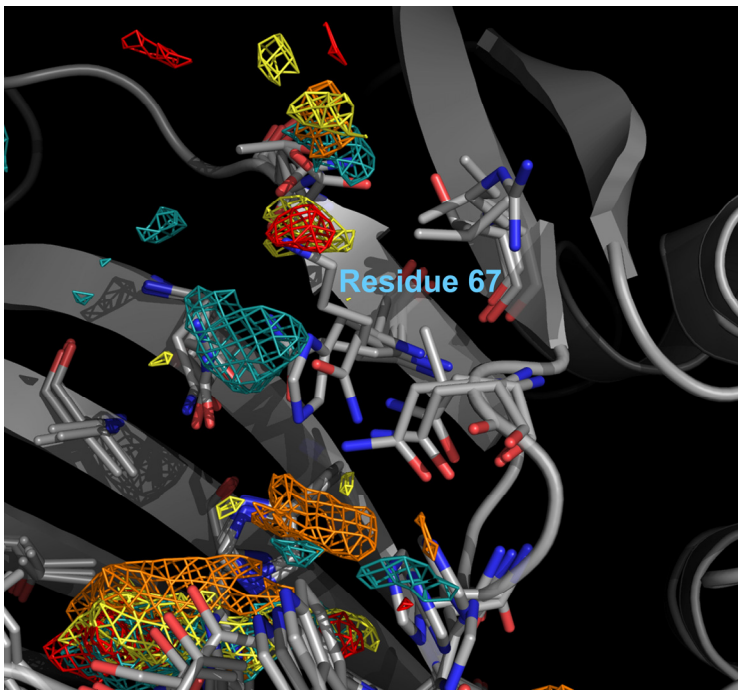

Figure S8. Molecular interaction fields of HBA probe (O) around residue 67 of carbonic anhydrase (hCA I - His, hCA II - Asn, hCA IX - Gln, hCA XII - Lys), depicted on isocontour level of –6.2 kcal/mol. Color of fields: hCA I - red, hCA II - orange, hCA IX - yellow, hCA XII - blue.

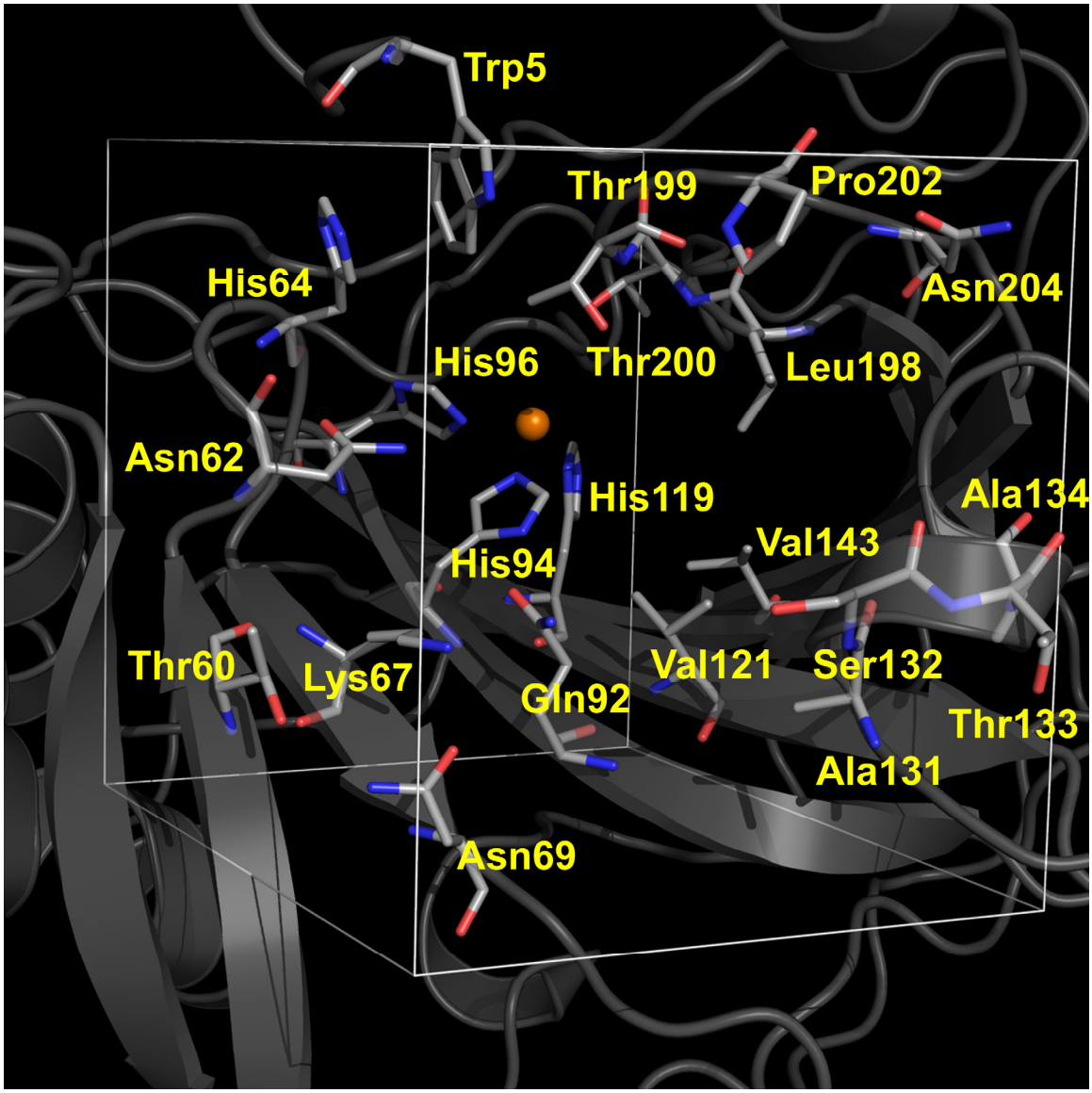

Figure S9. Labeled residues within the box used for GRID molecular-interaction fields calculation, exemplified on the hCA XII (PDB entry 1JD0). Active site Zn^{2+} ion is depicted as an orange sphere.

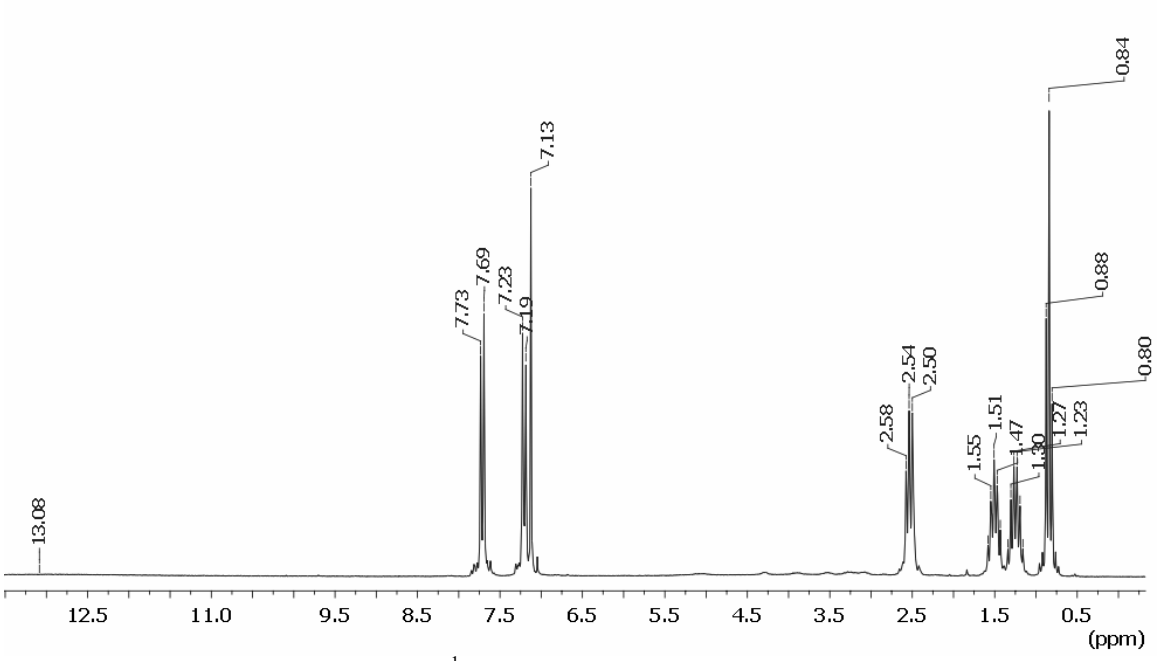

Figure S10. [1]H NMR spectrum of compound **4**.

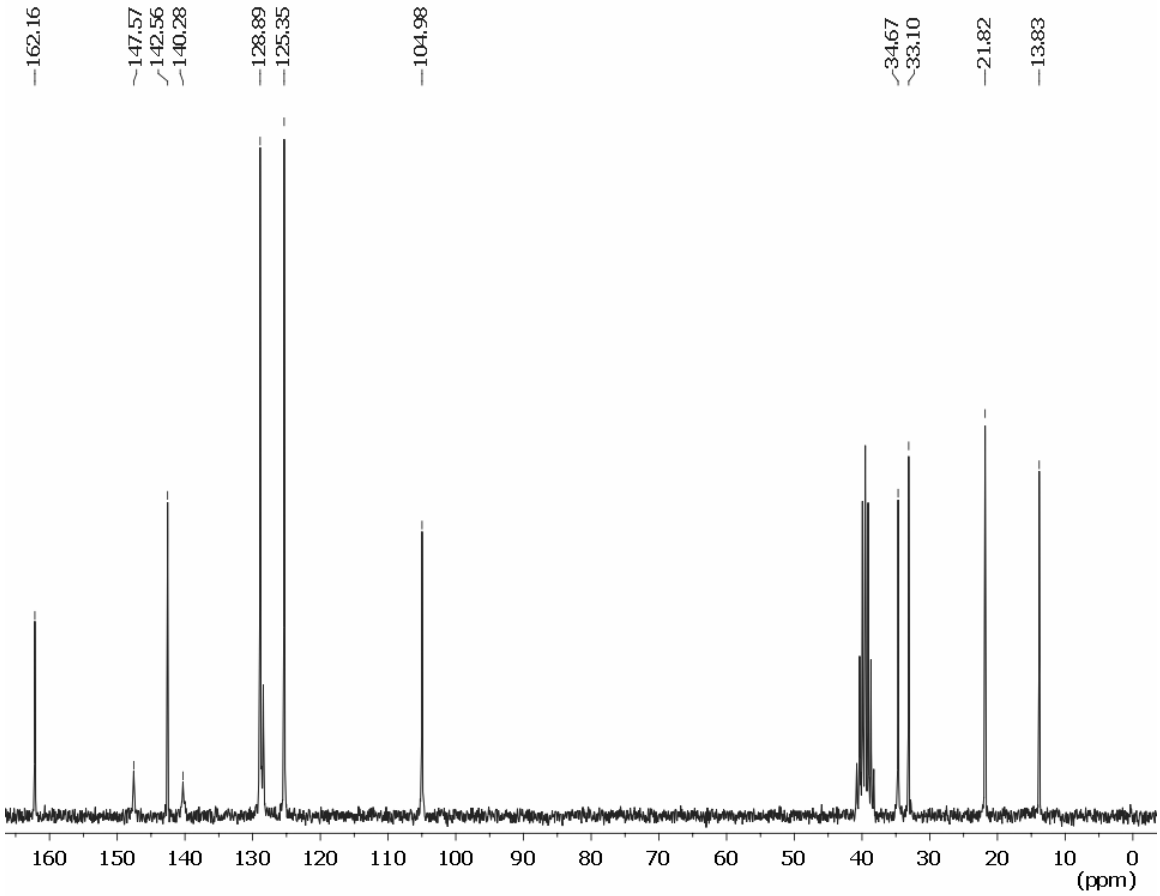

Figure S11. [13]C NMR spectrum of compound **4**.

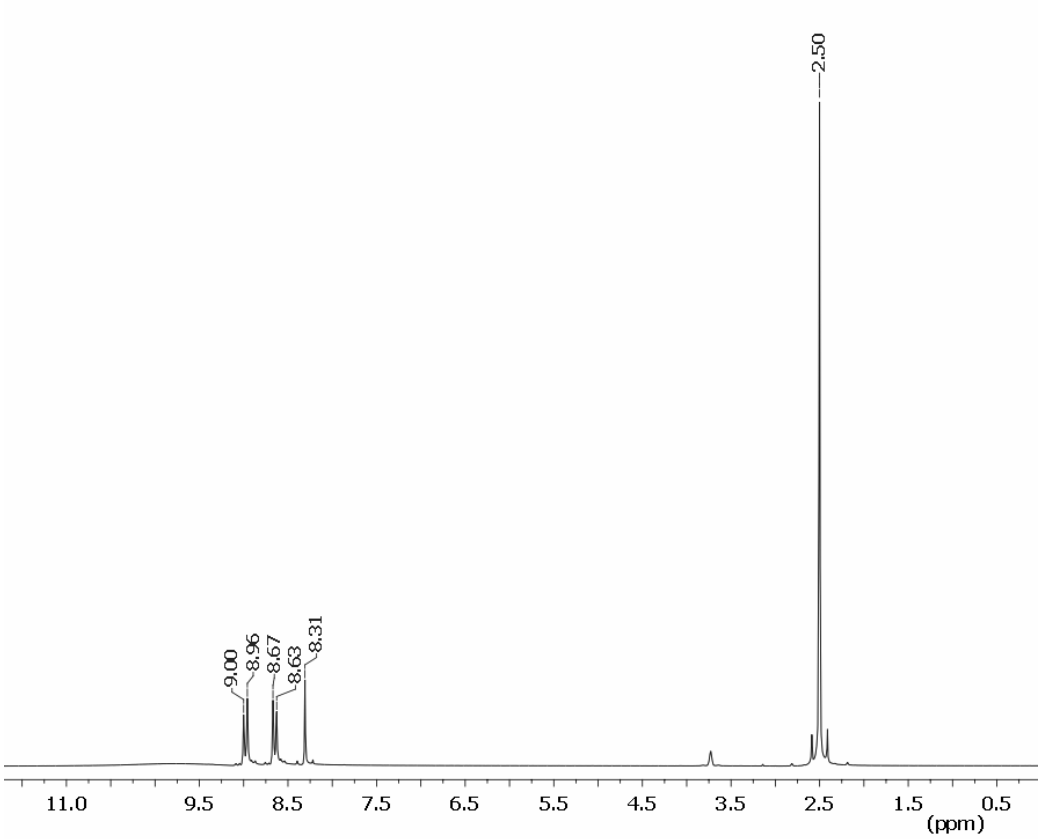

Figure S12. ^{1}H NMR spectrum of compound **5**.

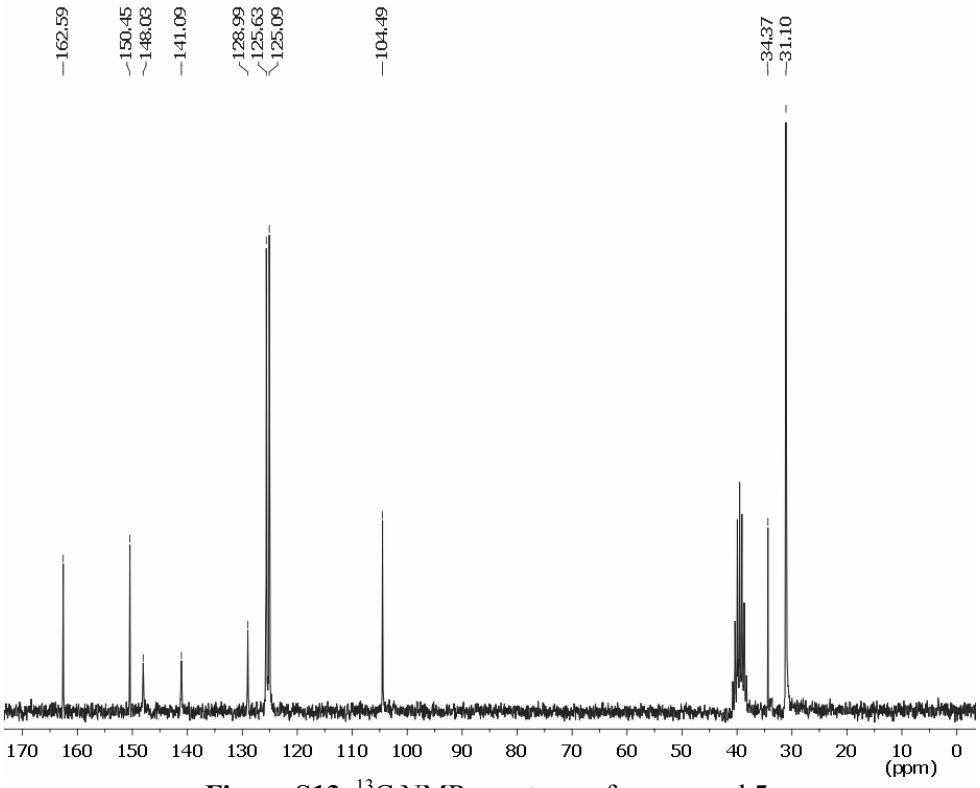

Figure S13. ^{13}C NMR spectrum of compound **5**.

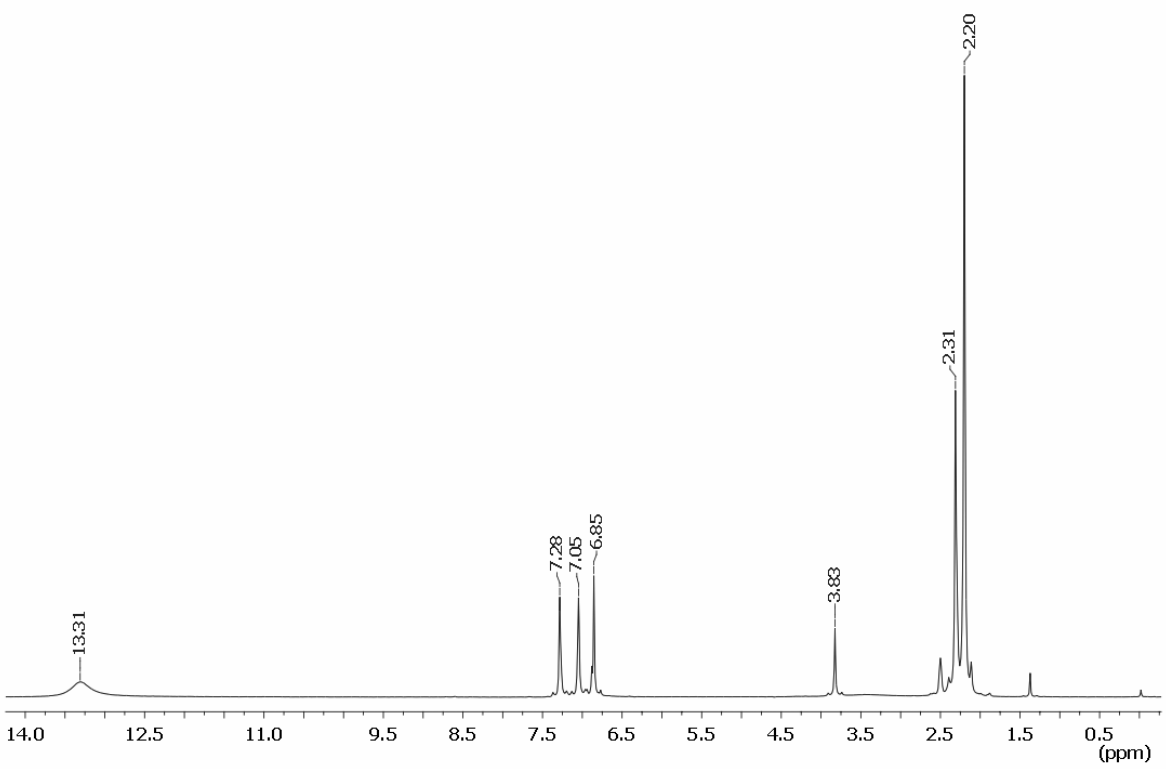

Figure S14. ^{1}H NMR spectrum of compound **8**.

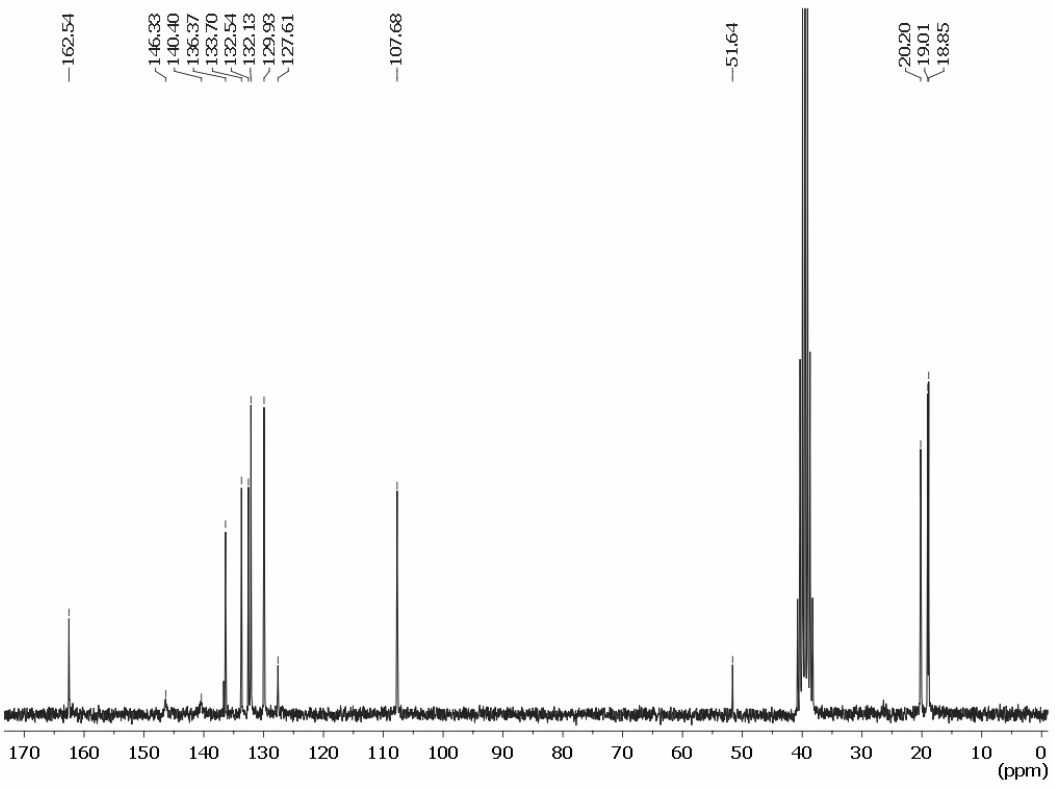

Figure S15. ^{13}C NMR spectrum of compound **8**.

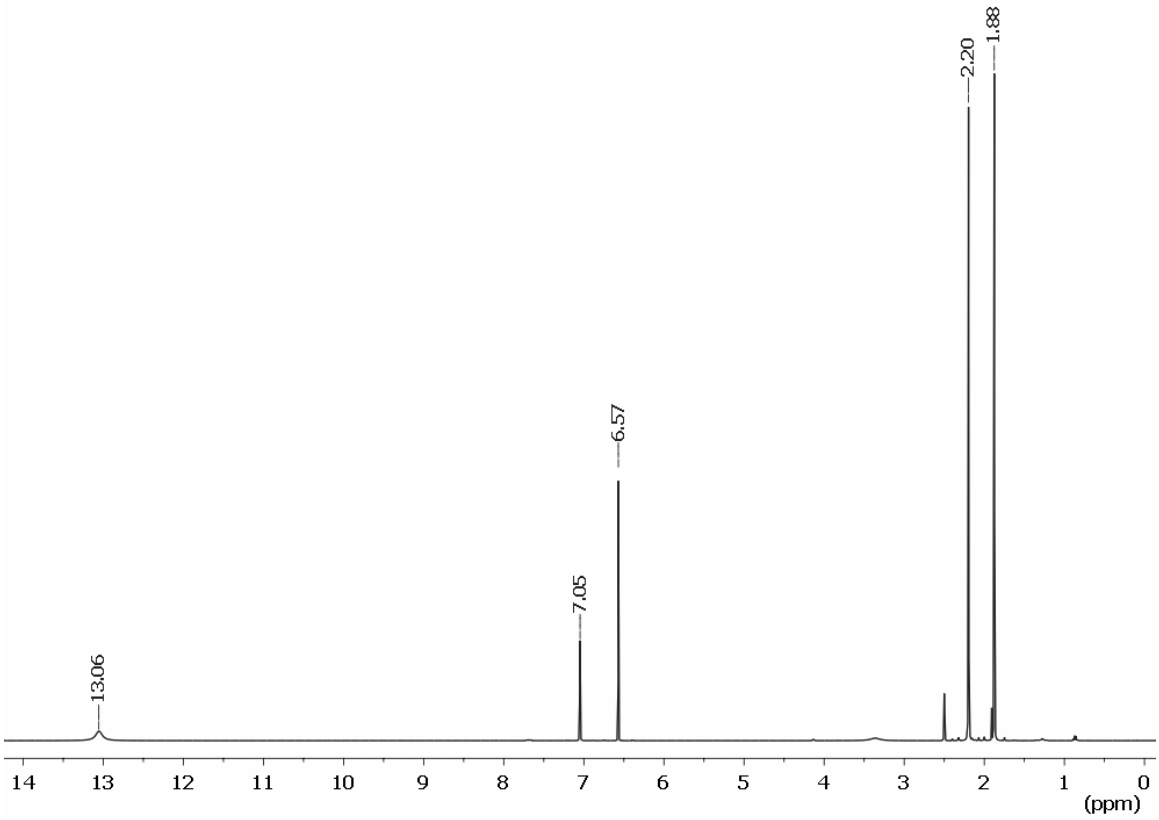

Figure S16. ^{1}H NMR spectrum of compound **9**.

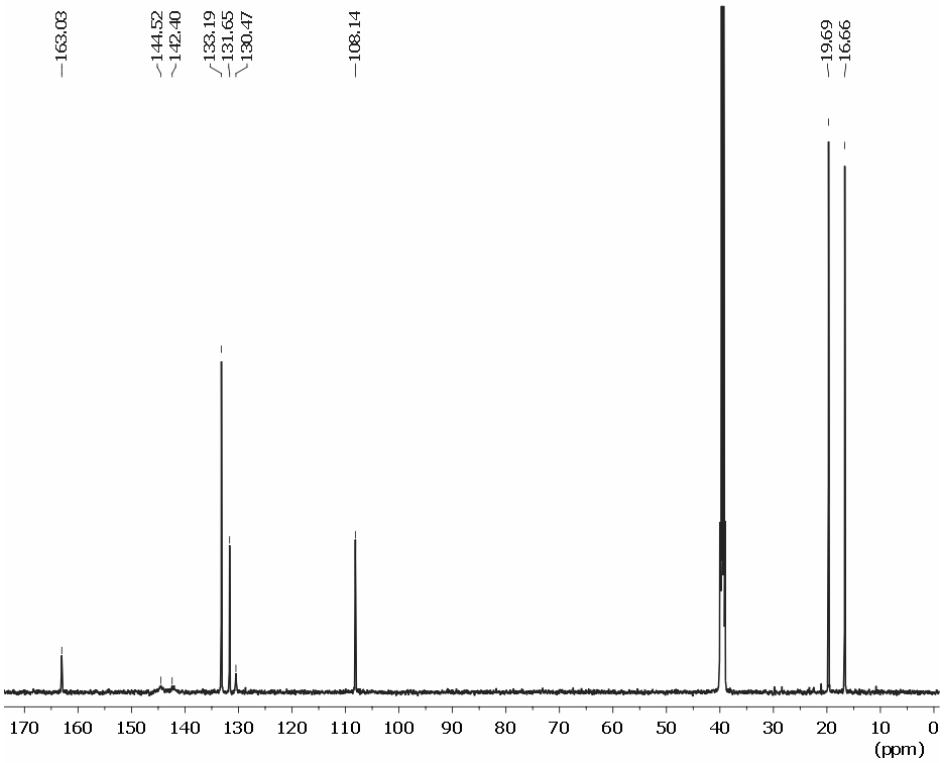

Figure S17. ^{13}C NMR spectrum of compound **9**.

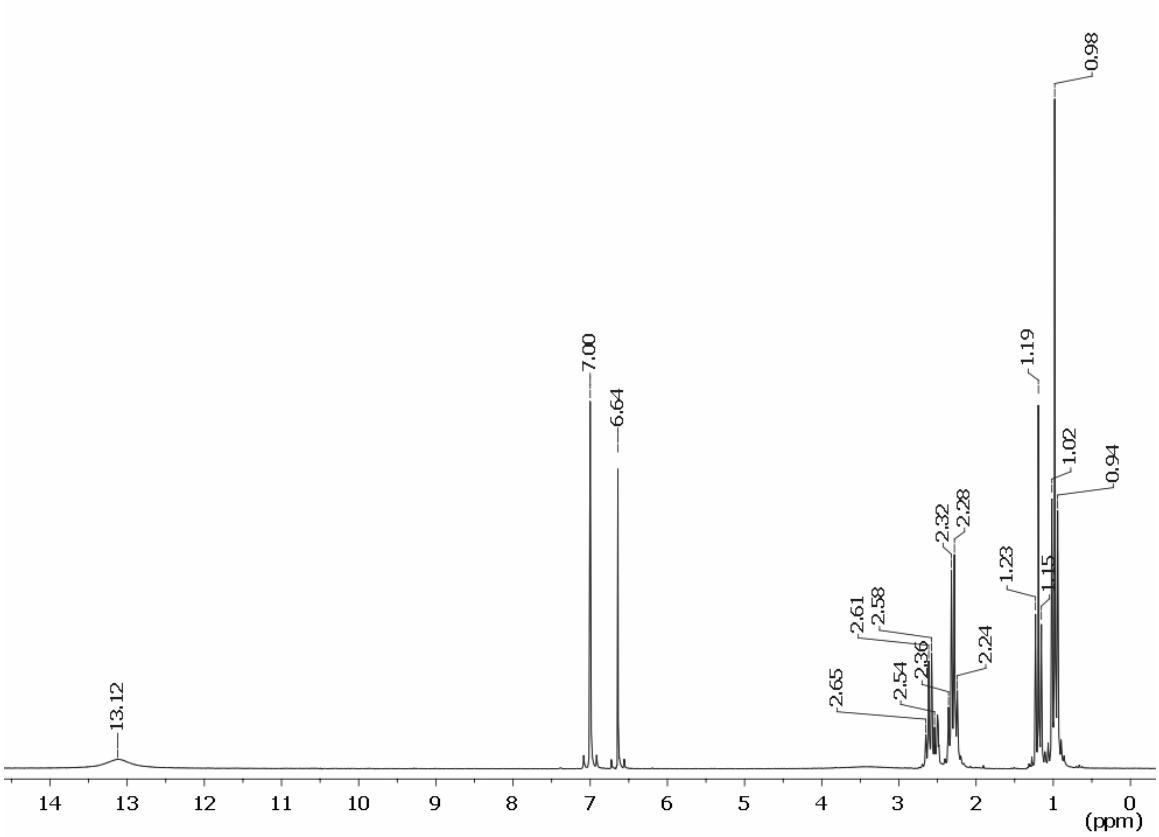

Figure S18. ^{1}H NMR spectrum of compound **10**.

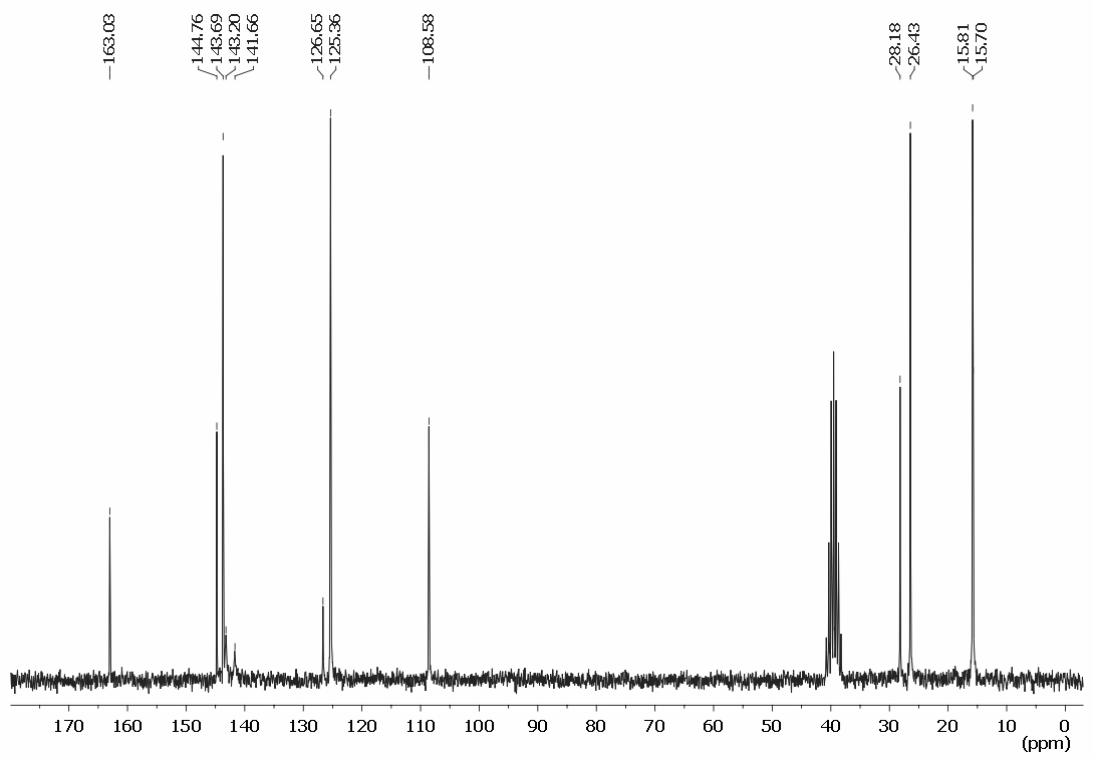

Figure S19. ^{13}C NMR spectrum of compound **10**.

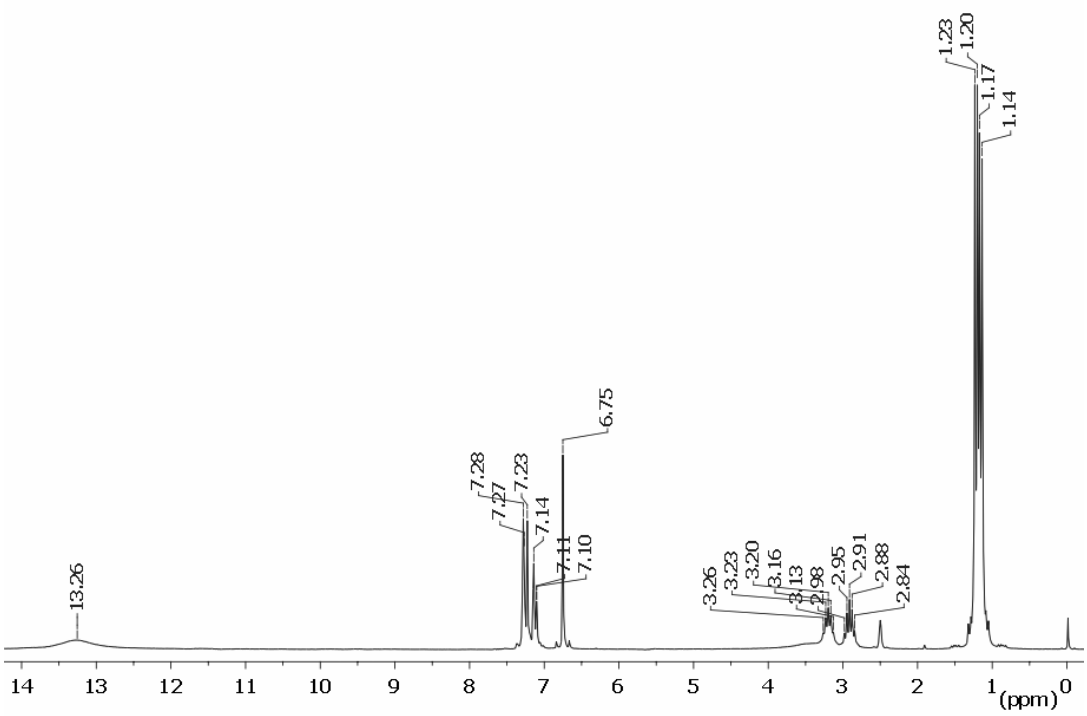

Figure S20. ^{1}H NMR spectrum of compound **11**.

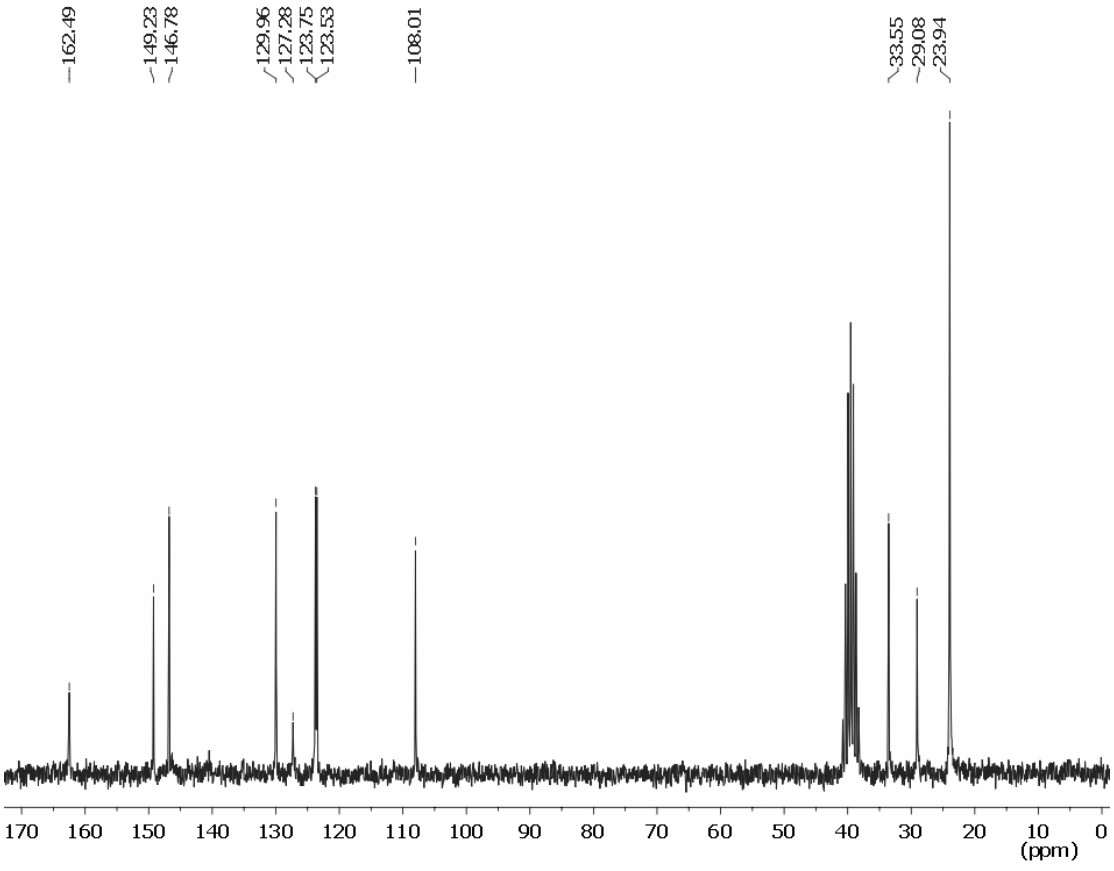

Figure S21. ^{13}C NMR spectrum of compound **11**.

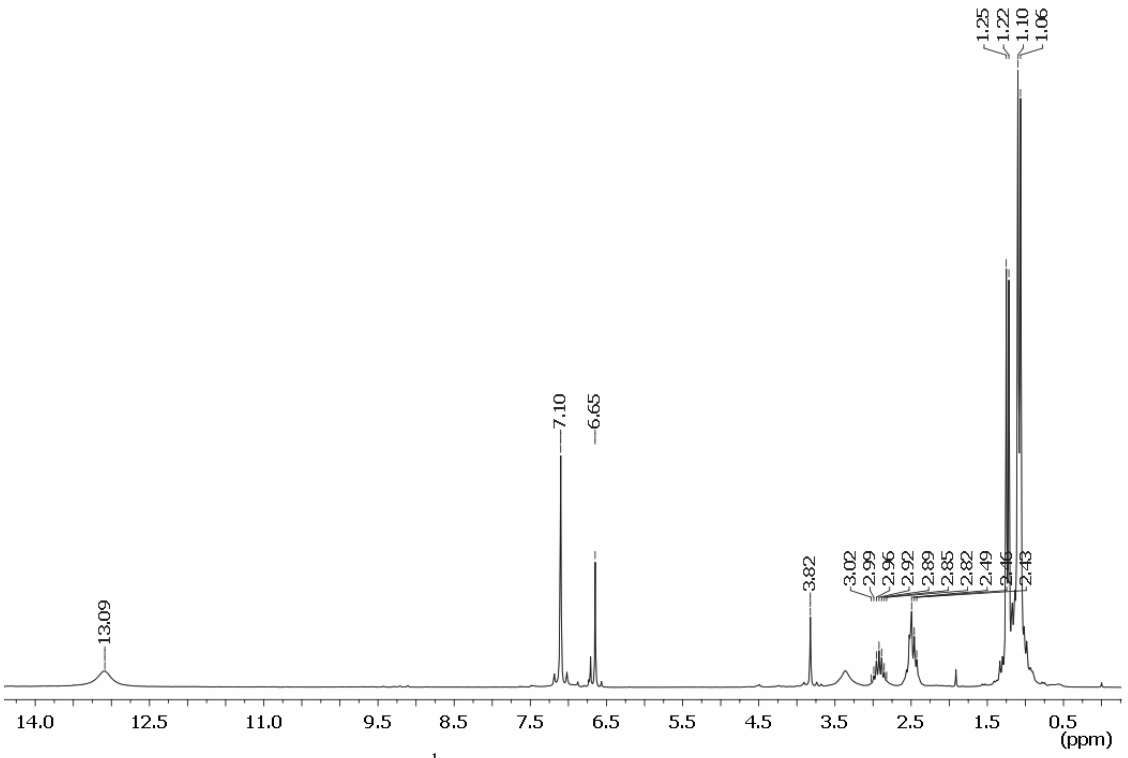

Figure S22. ^{1}H NMR spectrum of compound **12**.

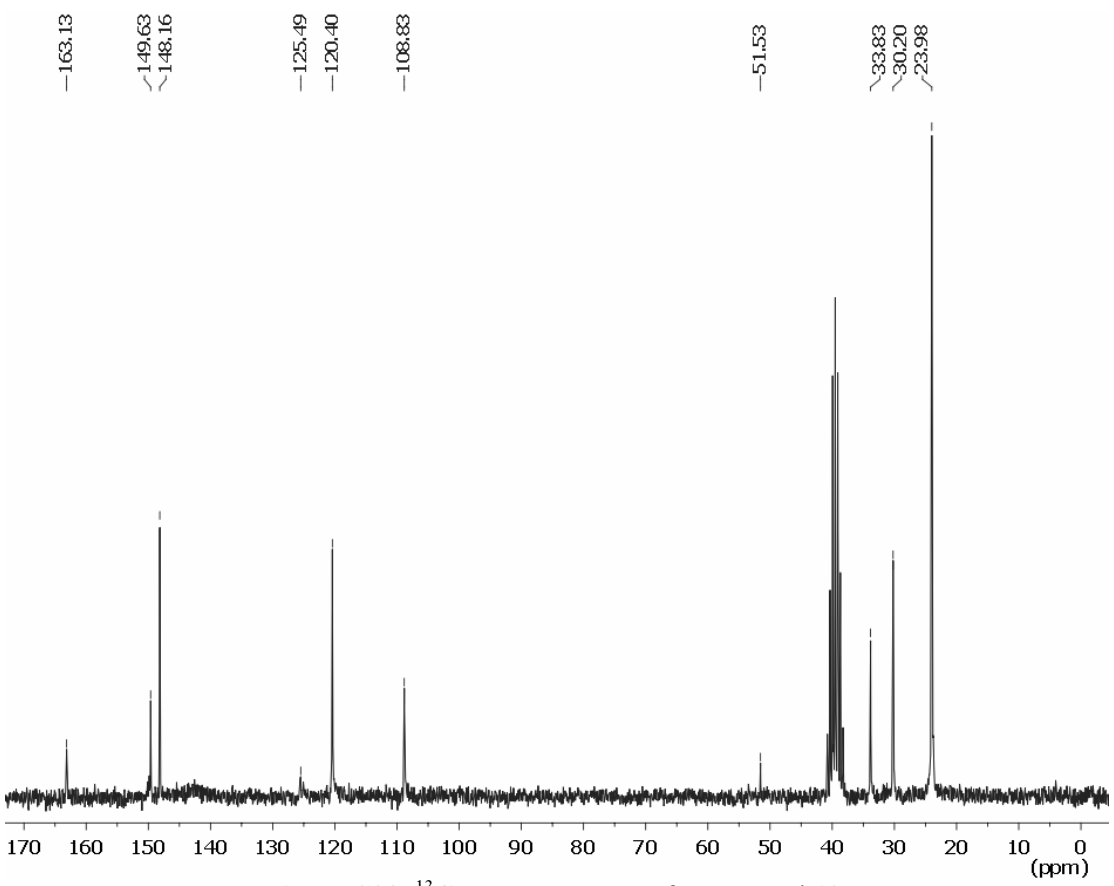

Figure S23. ^{13}C NMR spectrum of compound **12**.

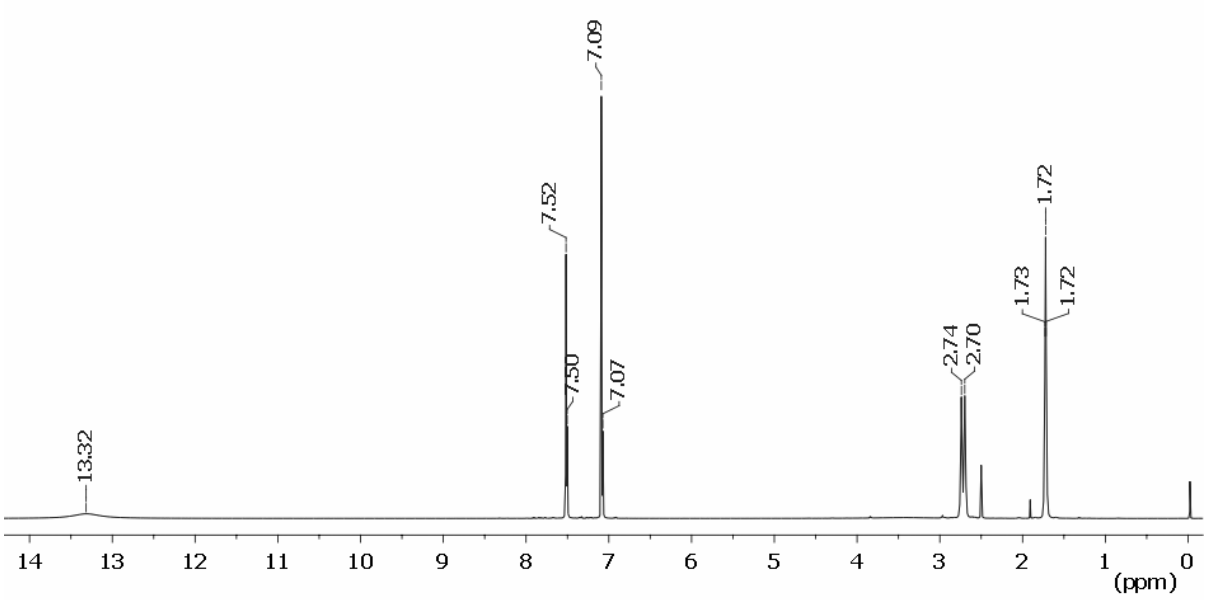

Figure S24. ^{1}H NMR spectrum of compound **13**.

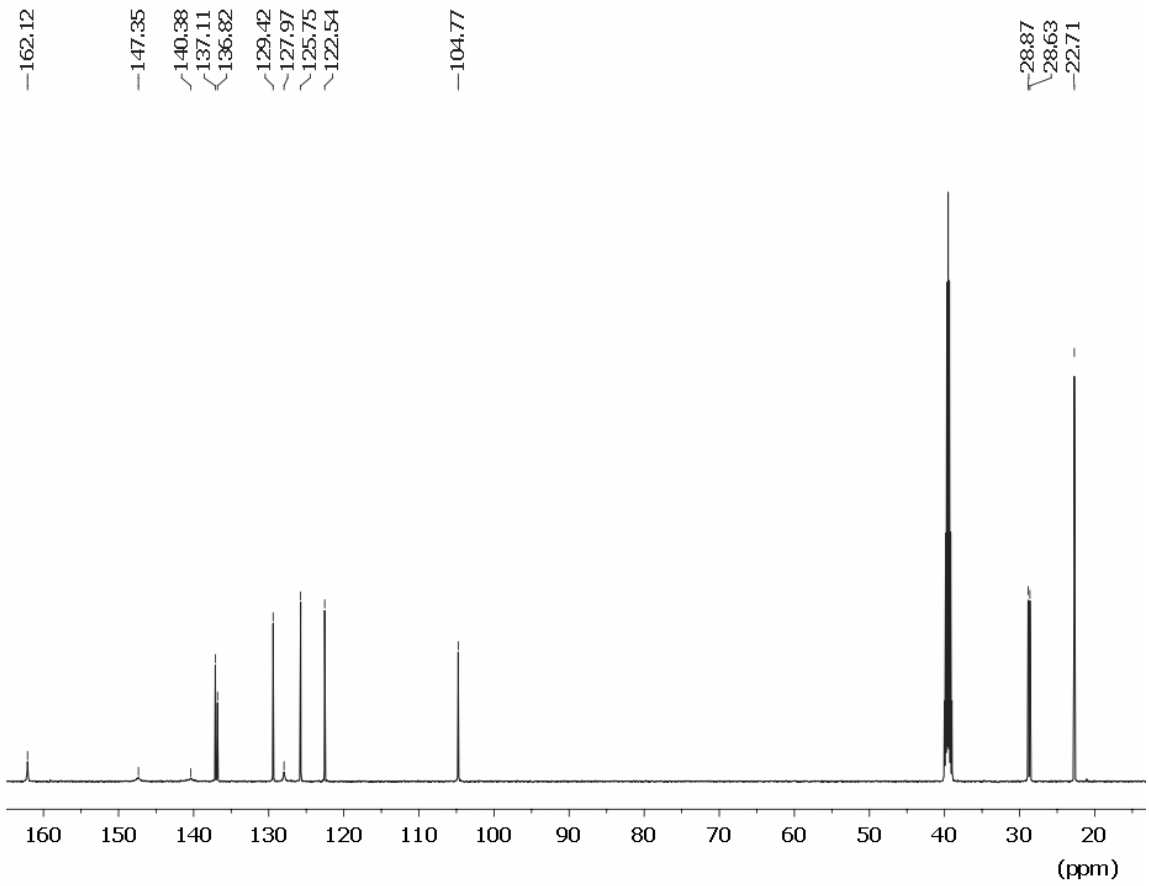

Figure S25. ^{13}C NMR spectrum of compound **13**.

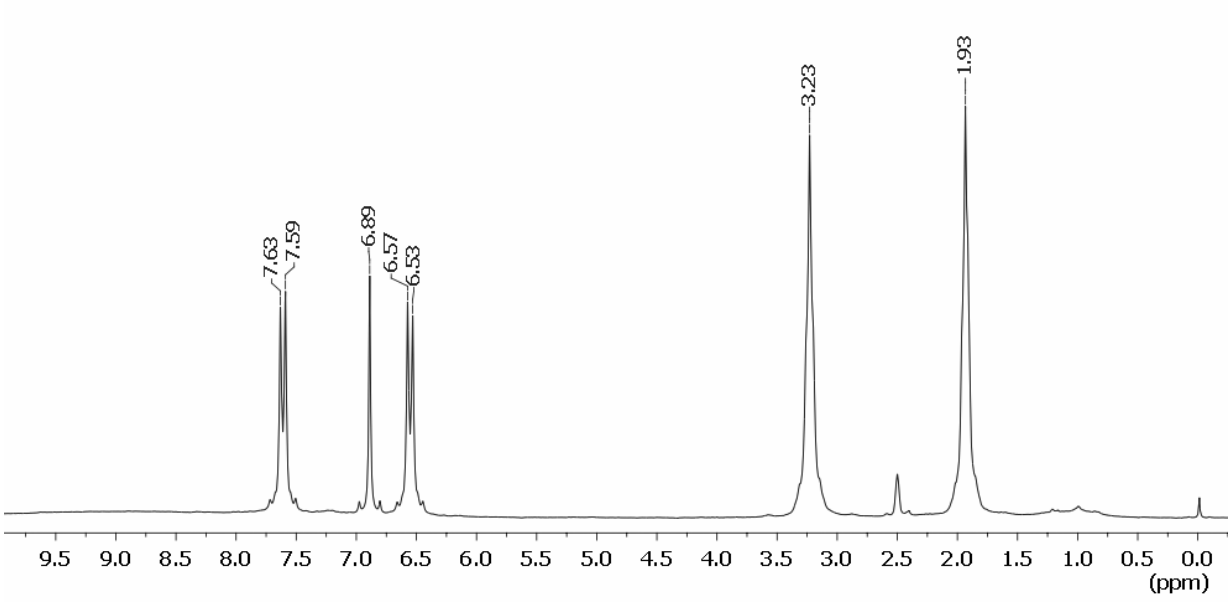

Figure S26. ^{1}H NMR spectrum of compound **16**.

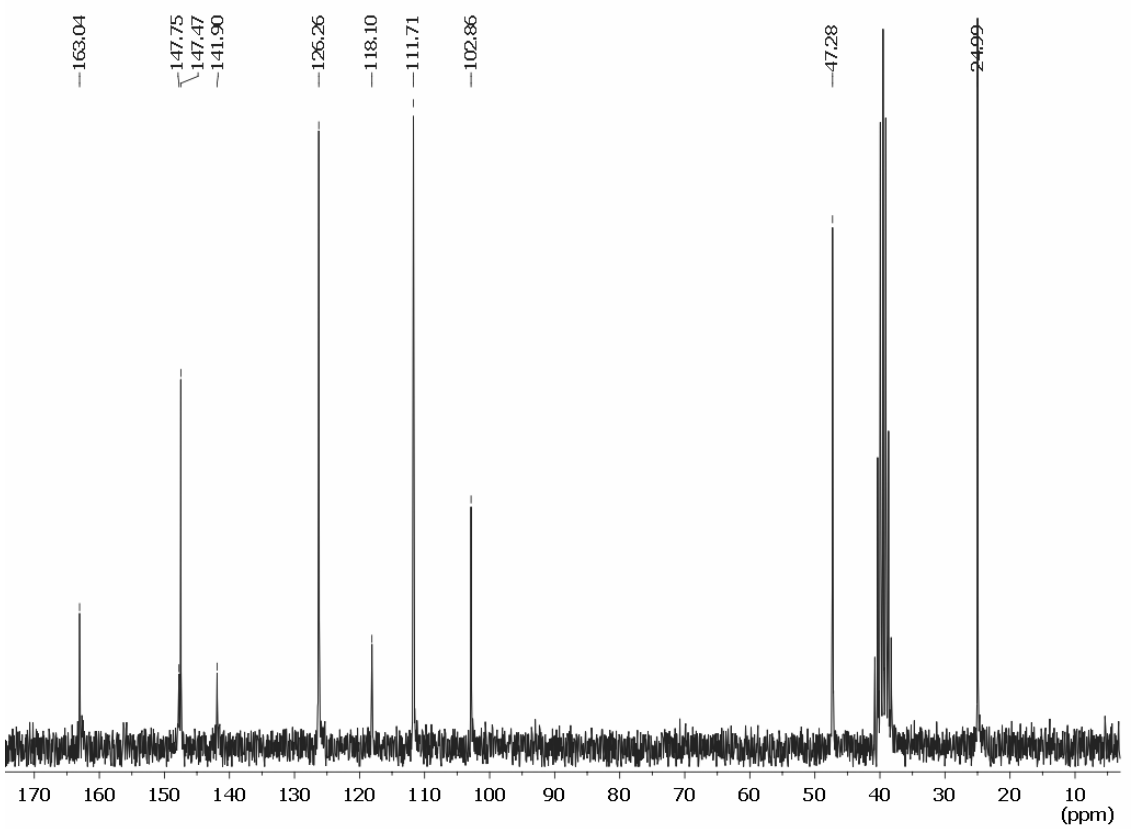

Figure S27. ^{13}C NMR spectrum of compound **16**.

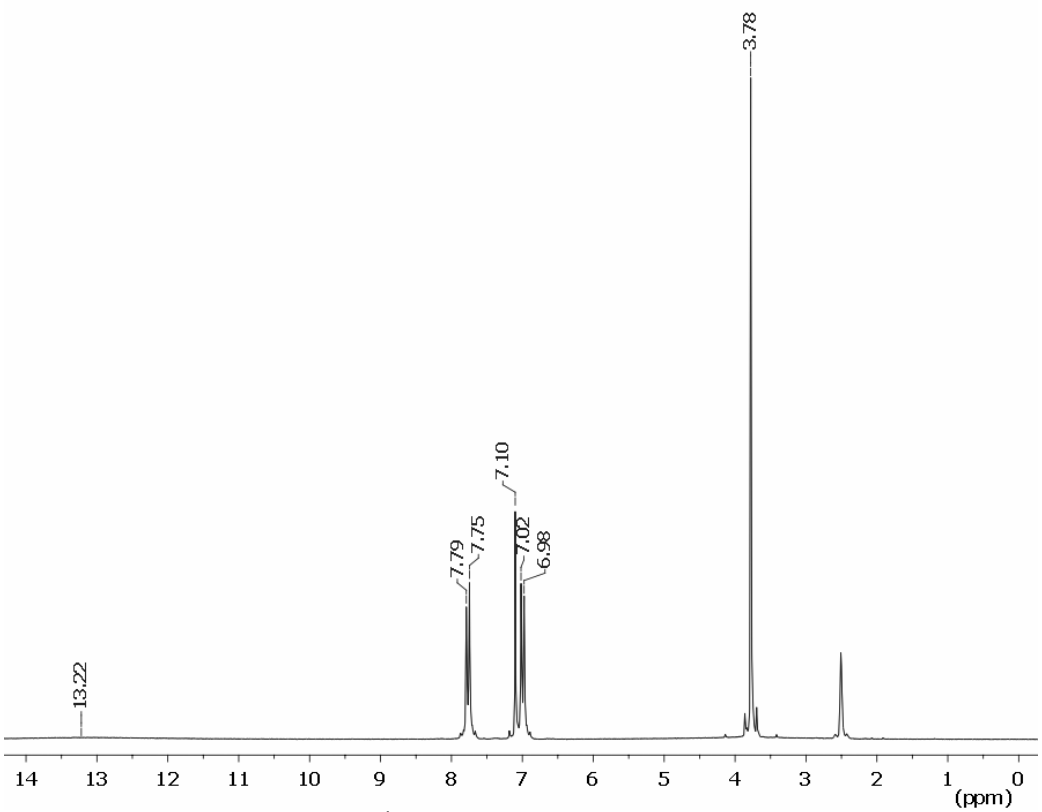

Figure S28. ^{1}H NMR spectrum of compound **22**.

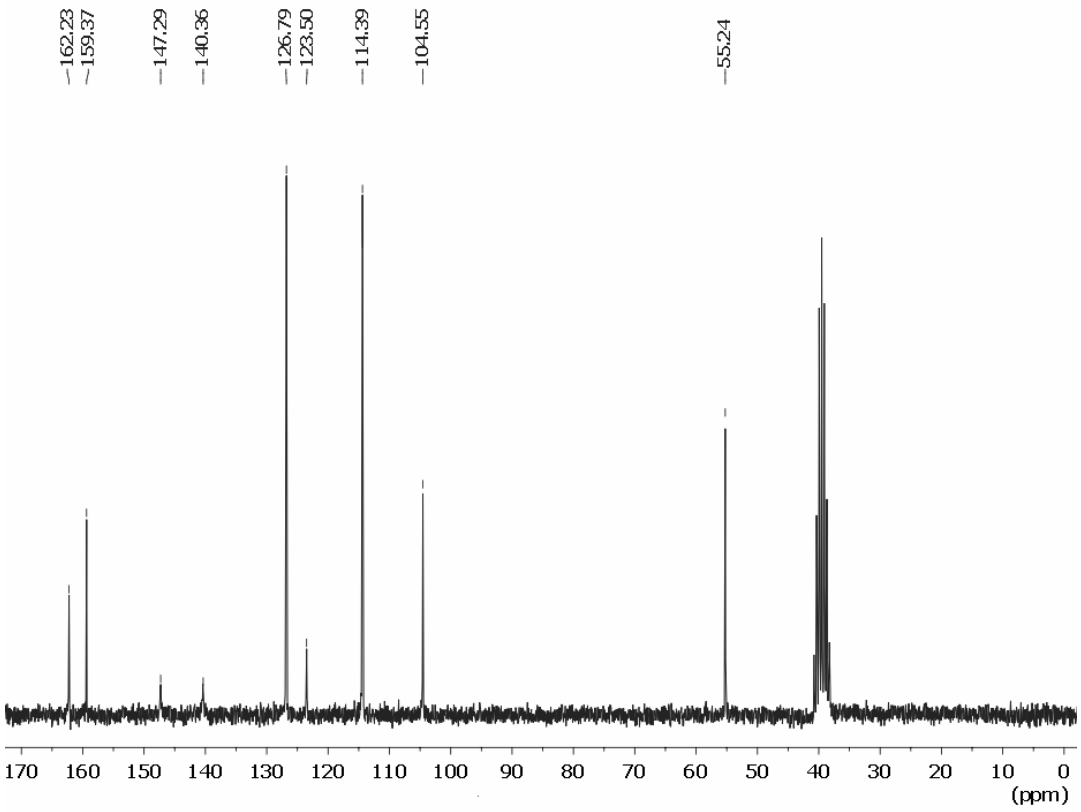

Figure S29. ^{13}C NMR spectrum of compound **22**.

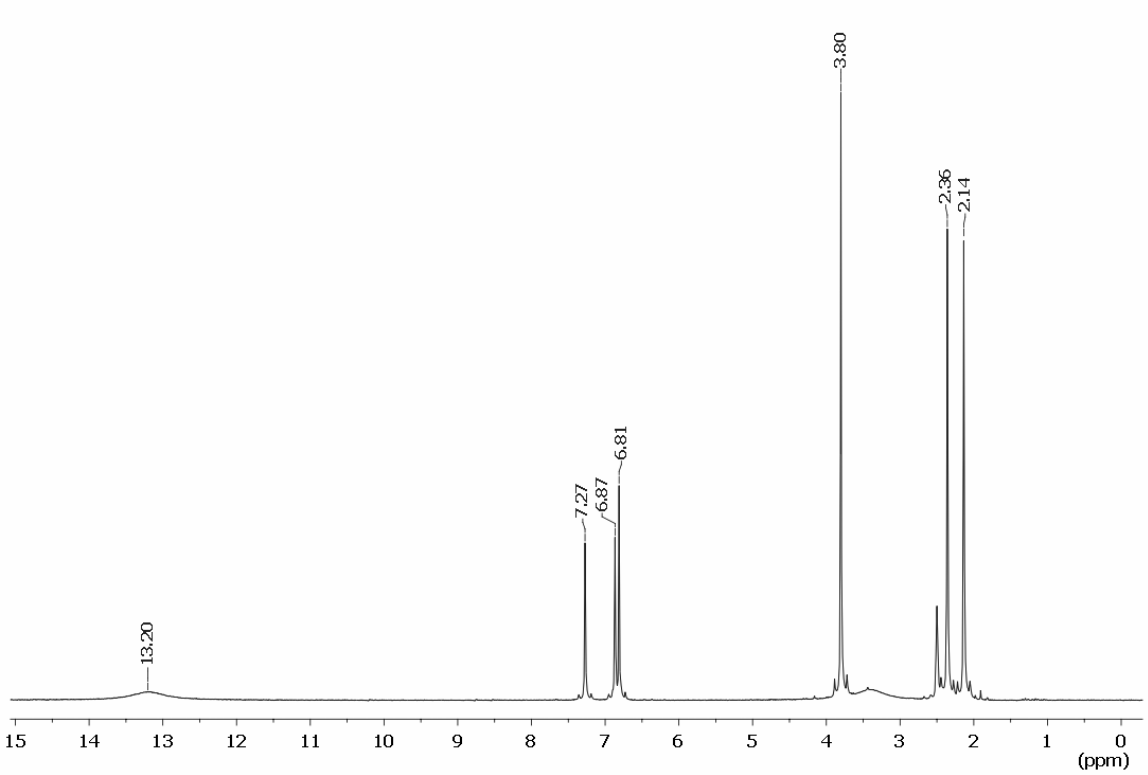

Figure S30. ^{1}H NMR spectrum of compound **23.**

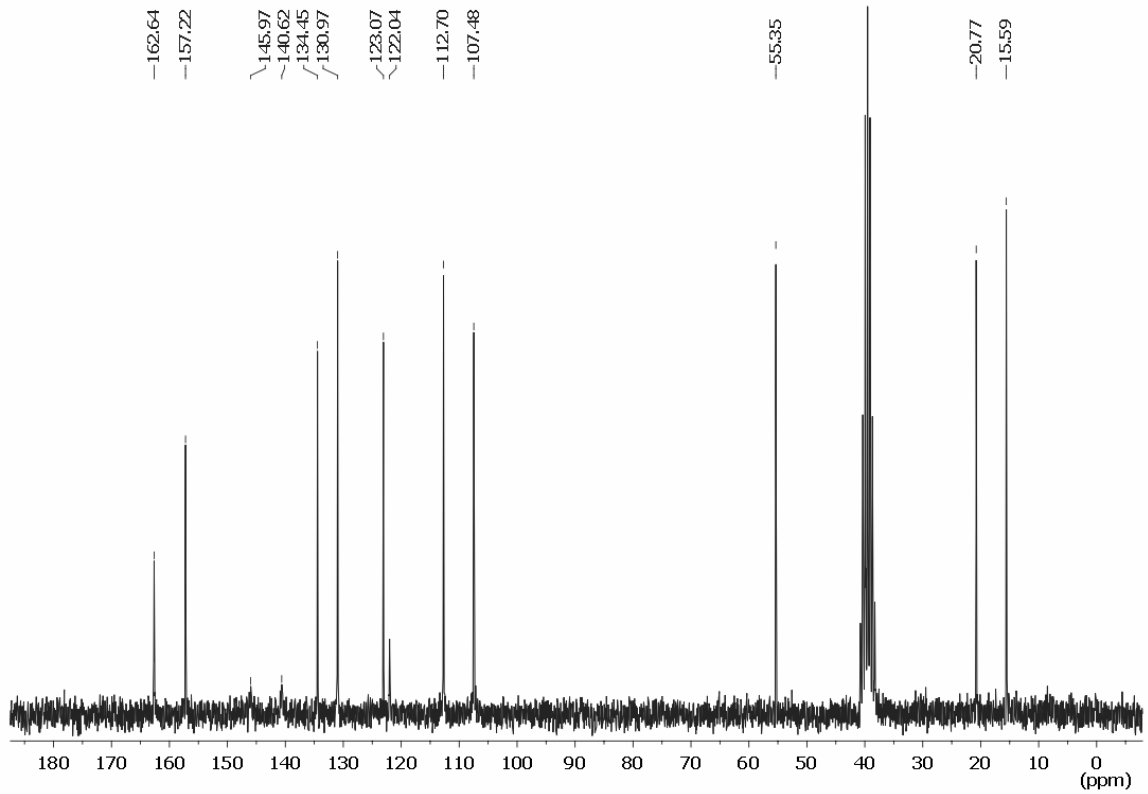

Figure S31. ^{13}C NMR spectrum of compound **23.**